JKAU: Sci., **Vol. 23** No. 2, pp: 3-15 (2011 A.D./1432 A.H.)
DOI: 10.4197 / Sci. 23-2.1

Characterization and Transport Properties of Indium Sesquitelluride Monocrystals

F. S. Bahabri* and **R. H. Al-Orainy**

Physics Department, Faculty of Sciences for Girls,
King Abdulaziz University, Jeddah, Saudi Arabia

Abstract. In the present study, single crystals of defect semiconductor In_2Te_3 were grown by the Bridgman technique. An investigation was made on the Hall effect, electrical conductivity and thermoelectric power of In_2Te_3 monocrystal in wide temperature range. The investigated samples were p-type conducting. The Hall coefficient yields a room-temperature carrier concentration of 7.8 $x10^9 cm^{-3}$. The band gap was found to be Δ Eg = 0.99 eV. Hence a combination of the electrical conductivity and Hall effect measurements enable us to study the influence of temperature on the Hall mobility and to discuss the scattering mechanism of the charge carriers. Also the present investigation involves thermo -electric power measurements of In_2Te_3 single crystals, These measurements enable us to determine many physical parameters such as carriers mobilities, effective masses of free charge carriers, diffusion coefficients, diffusion length, as well as relaxation time. Also the figure of merit was determined.

1-Introduction

In recent years a great deal of interest has been focused on semiconducting III-VI compounds, as a collective group of materials have been and are still the subject of much intensive investigation. In the last few years widespread attention has been paid to the semiconductors of the (A^{III} B^{VI}) group. This interest has been driven by their possible device applications [1].Great attention has been paid [2] to Ga, In - and Te

* Corresponding Author: Tel.:+966 2 6728584; Fax: +966 2 6756862.
E-mail: f_s_bahabri@hotmail.com

– chalcogenides. In particular the study of $A_2^{III} – B_3^{VI}$ compounds is quite attractive. Binary chalcogenide alloys $A_2^{III} B_3^{VI}$ (A = Al, Ga, In, and B = S, Se, Te) with semiconducting properties have been widely studied during the last few decades[3]. Indium tellurides are useful as materials for electronics and for optical recording. The phase diagram of the In- Te system studied by many autors[4-7]. The In_2Te, In_9Te_7, In_4Te_3, InTe, In_3Te_4, α – In_2Te_3 (low temperature), β – In_2Te_3 (high temperature), In_3Te_5, In_4Te_7 and In_2Te_5 compounds were claimed to be formed in the In –Te system under standard conditions. The existence of In_2Te, In_9Te_7, In_3Te_4 and In_4Te_7 phases are questionable. Among these compounds, In_2Te_3 which is interesting for its photoconduction properties(8.9) and also for its switching and memory effects[10,11], is found to have two modifications labelled as α and β corresponding to low and high temperature formation, respectively. Crystallographic and band structures[12,13], lattice vibration[14,15], ordering and defects[16,17], and also optical[18], electrical and photoconducting properties[8,9,18] of this semiconductor have been studied. Thus the fundamental properties of In_2Te_3, in particular the transport properties of In_2Te_3, still remain unknown. The reason is that there is a Lake of high- quality single crystals available for the experiments. The present investigations on electrical conductivity, Hall coefficient and thermoelectric power of In_2Te_3. It is essential to the understanding of the materials and consequently of their practical applications.

2-Experimental

2-1-Preparation of Sample

The apparatus and procedure for crystal growth are mainly the same as those described by Hussein and Nagat[19],in previous work. In_2Te_3 samples were prepared using a modified Bridgman technique for growing crystal from melt. Indium sesquitelluride monocrystals were prepared from high purity indium (6N) representing 37.496% and Tellurium (5N) representing 62.504%. The single crystallinity of this material was checked using the X-ray diffraction technique. Diffraction for these materials compared with the index data of the American Society for testing materials (ASTM) cards. From these X- ray studies it was evident that the crystal has a high degree of crystallinity, indicating that the preparation technique is fairly reliabe and satisfactory, since the

results indicated that the ingot was good crystalline material with the required phase without any secondary phases.

2-2-Experimental Arrangement

Measurements of the electrical conductivity and Hall effect were done with the help of a Pyrex glass cryostat, which was designed by Hussein[20] for this purpose. The cryostat is used as a holder, evacuated container for liquid nitrogen (for low- temperature measurements) and a support to the electric heater (for high- temperature measurements). Using an Edward rotary pump, for evacuated the crystal. Copper – constantan thermo-couple was used for measuring the temperature of the sample. Silver paste was used for the ohmic contact. Specimens were ground and polished thoroughly with the use of diamond pastes to obtain mirror- like surfaces. Typical dimensions for rectangular sample were (8.5 x 2.7 x 1.3 mm^3). The Hall measurements were made in a magnetic field of 0.7 Tesla and were performed using the conventional D.C potentiometer method. For thermoelectric power (TEP) measurements, an evacuated calorimeter was used to protect the sample from oxidation and water vapor condensation at high and low temperatures respectively. The calorimeter was built with two heaters. The outer heater found the external source and discharged its heat slowly to the specimen environment. The inner heater was attached to the lower end of the crystal in order to control the temperature and its gradient along the specimen. Two copper-constantan thermocouples were used for the temperature measurements a cross the two ends and the thermo-EMF in the sample was measured from one of their arms. The thermo-EMF was measured relative to the copper. More details about the apparatus, and experimental techniques were previously published by Hussein it al[21].

3-Results and Discussion

3-1-Temperature Dependence of Electrical Conductivity and Hall Effect for In_2Te_3

Figure 1 shows the variation of electrical conductivity σ versus inverse temperature for In_2Te_3 single crystal. The complete temperature range can be subdivided into three regions, below the transition,the transition region and above the transition.

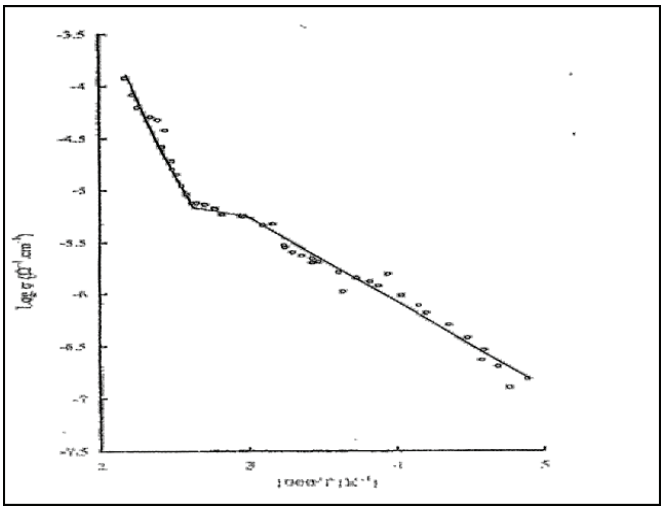

Fig. 1. The temperature dependence of electrical conductivity (σ) for In2 Te3 single crystal.

These regions are quite clearly shown in fig.1. With increase of temperature the electrical conductivity at first increases, then it reaches the transition region at 335 K, then the lg σ vs. 1/T curve passed through an intermediate region (335-370 K) in which the carrier concentration is not actually constant, and in the third region, σ rises again. This pattern of changes in the electrical conductivity is due to the appearance of impurity and intrinsic conductivity, respectively, and to the variation of the hole mobility and concentration with temperature. In the intermediate region where the carrier density ($N_A - N_D$ = constant), until the intrinsic region is reached. At temperatures above the transition point the conductivity increases rapidly. The temperature dependence exhibits a transition from a region of lower slope to one of higher slope. The slopes of the curve increase with increasing temperature, and are higher at higher temperature because of the carriers being excited from the extended state of the valence band into the conduction band. The width of the forbidden gap as calculated from the slope of the curve in the high-temperature region is found to be ΔEg = 0.99 eV. The room temperature conductivity of In_2Te_3 singly crystal equal to ($2.5x10^{-6}$ $\Omega^{-1}cm^{-1}$). The Hall coefficient (R_H) variation with temperature and a positive sign of (R_H) indicated the major contribution to the conductivity by holes. Figure 2 shows the temperature dependence of ($R_H T^{3/2}$), it is the usual type for semiconductors. Assessment of the forbidden- band width from this

graph have found a value close to that determined from electrical conductivity and that reported by Guizzeffi et al[22].

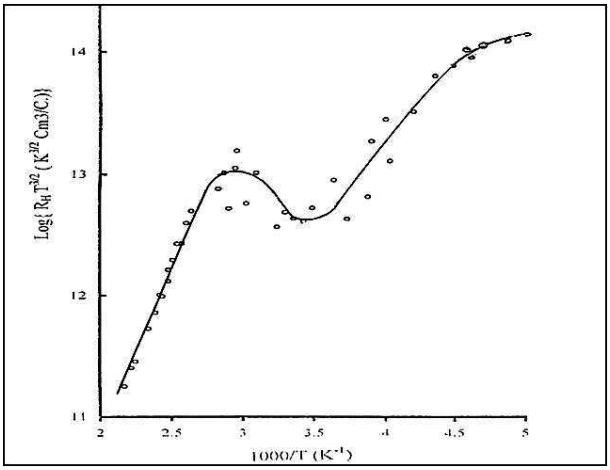

Fig. 2. The dependence of RH T3/2 against the temperature for In2 Te3 single crystal.

It was found also the depth of the acceptor center is 0.3 eV. The variation of Hall mobility with temperature is shown in Fi.3.

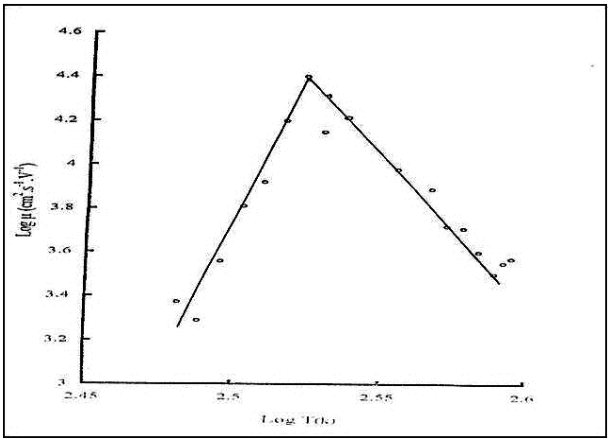

Fig. 3. The variation of the Hall mobility with temperature for In2Te3 single crystal.

It was found that the exponent (n) in the relation $\mu \sim T^n$ below 340 K, is equal to 23 and increases with temperature, while in the high temperature range (T > 340 K) the mobility decreases according to the

low $\mu \sim T^{-13}$ from this relation, it seems that the value of n is unusually large compared with those obtained for impurity and lattice scattering respectively in other semiconductors. This behavior, in our opinion may be associated with the presence of a high density of stoichiometric vacancies and the creation of defects. The exact nature of defects in these semiconductors remains uncertain[23], but from structural considerations and also by analogy with III –V compounds, vacancies and anti-site defects are likely to play an important role, stoichiometric cation vacancies present are themselves not neutral but their presence is responsible for the easy restoration of radiation ejected atoms into lattice sites across low energy barriers. The room temperature value of the mobility was found to be 1820 cm^2 / V.sec. The variation of carrier concentration with temperature is shown in Fig.4.

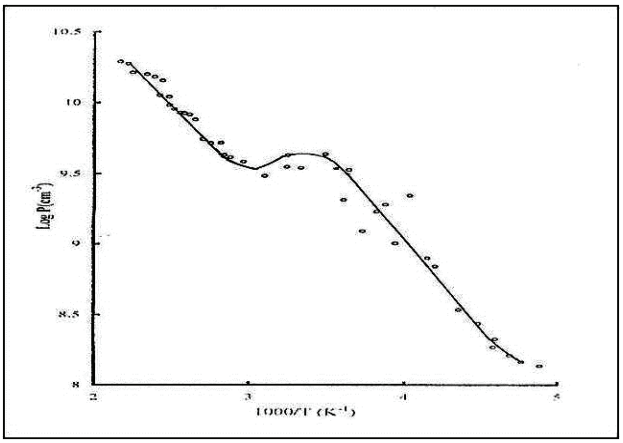

Fig. 4. The variation of carrier concentration with temperature for In2 Te3 single crystal.

As the In_2Te_3 sample is exhibiting intrinsic behavior above 370 k the expected value for the intrinsic concentration will be given as:

$$n_i = 2\left(\frac{2\pi K}{h^2}\right)^{3/2}\left(m_n^* m_p^*\right)^{3/4} T^{3/2} \exp(-\Delta Eg / 2KT) \qquad (1)$$

Where, K is the Boltzman constant, T is the temperature, ΔE_g is the energy gap width and (m_n*, m_p*) are the effective masses of electrons and holes respectively. One can see that the carrier concentration varies sharply with increasing temperature. The room temperature concentration is 7.8 x109 cm^{-3}.

3-2- Temperature Dependence of TEP for In2 Te3 Single Crystal

The thermoelectric power (TEP) measurements were performed in a wide temperature range (180-500 K).

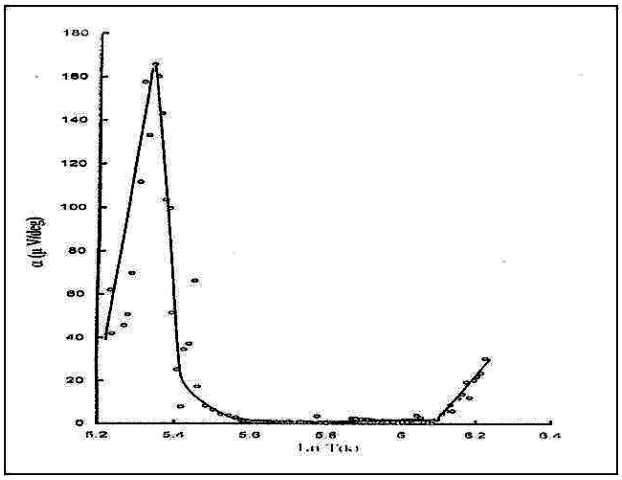

Fig. 5. Temperature dependence of TEP for In_2 Te_3 single crystal.

Figure 5 illustrates the general mode of variation of TEP with temperature. This was done by plotting the relation between α and ln T. Some features of these results may be pointed out: (1) The thermoelectric power grows monotonically with temperature and shows a sharp maximum at value of α 160 μV/K at T corresponding to 209 K. (2) With further rise in temperature a rapid fall in thermal emf is noticeable and a minimum is observed at 270 K. (3) With further rise in temperature, decreases but very slowly. (4) At temperature higher than 440K, the magnitude of α rises and the relation is clearly linear.(5) It is evident from the result In2Te3 samples have positive TEP in the entire temperature range indicating a p-type conductivity of the investigated samples, which is in qualitative agreement with our previous data of Hall coefficient. (6) The room temperature TEP value amounted to be 5 μV/K. As follows from the expression for TEP of a semiconductor in the intrinsic region[24].

$$\alpha = -\frac{K}{e}\left[\frac{b-1}{b+1}\left(\frac{\Delta E_g}{2KT}+2\right)+\frac{1}{2}\ln\left(\frac{m_n^*}{m_p^*}\right)^{3/2}\right] \qquad (2)$$

Where, K is the Boltzman constant, b is the ratio of the electron to hole mobilities, ΔE_g is the energy gap width and (m_n*, m_p*) are the effective

masses of electrons and holes respectively. Figure 6 shows the relation between the thermoelectric power and the inverse of temperature.

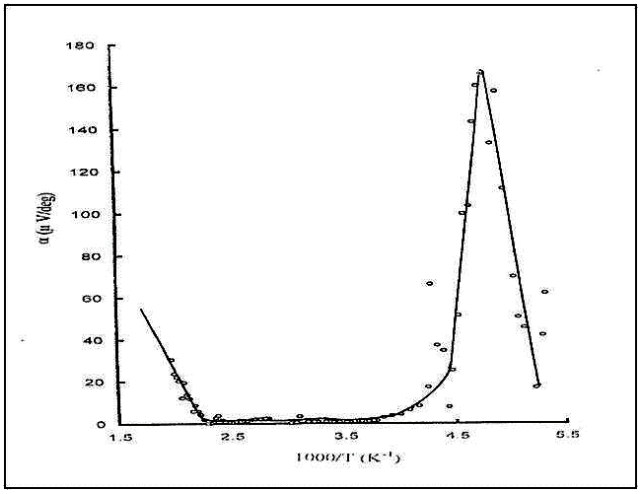

Fig. 6. Plot of (α) against 10^3 /T for In_2 Te_3 single crystal.

This relationship shows that a plot of in the intrinsic range, as a function of reciprocal of absolute temperature, is a straight line. The measured thermoelectric power in conjunction with the previously obtained Hall effect data are used to calculate electron to hole mobility ratio and also the ratio of effective masses of both electron and holes. The slopes of curve are used to estimate the ratio of the electron and hole mobilities. Taking ΔE_g = 0.99 eV, the ratio b = μ_n / μ_p is found to be 1.6. since μ_p = 1810 cm^2 /V.s, then we can evaluate μ_n = 2890 cm^2 /V.s. Another important parameter can be deduced with the aid of the obtained values of μ_n and μ_p using the Einstein relation, that is the diffusion coefficient for both majority and minority carriers at room temperature can be evaluated to be 47 and 75 cm^2 /s respectively. The ratio between the effective masses of both electrons and holes can be evaluated from the intersection of the curve. We evaluate this ratio as (m_n^* / m_p^* = 0.16). Figure 5 also shows a straight line relation in the low temperature region. A sharp drop of thermoelectric power is observed in the impurity region. In the impurity region the following formula could be applied:

$$\alpha = \pm \frac{K}{e}\left[2 - \ln\left(\frac{(n+,-)h^3}{2(2\pi\,(m^*_{+,-})KT)^{3/2}}\right)\right] \qquad (3)$$

Where the sign of α is the sign of the carriers (n $_{+}$, -) represents the number of free carriers (holes or electrons) respectively and (m^{*}_{+}, -) denotes the effective mass of holes or electrons respectively. Thus the effective mass of holes is evaluated to be 4.2 x 10^{-38} kg. Combining this value with the above – mentioned results for the ratio (m_n^{*} / m_p^{*}), one obtains an effective mass of minority carriers of the value m_n^{*} = 6.3 x10^{-39} kg. Using the effective mass values of electrons and holes, the relaxation time for both current carriers can be determined. Its value for holes comes to 4.5 x10^{-18} sec. Whereas for electrons it is equal to 1.2 x10^{-18} sec. By using the values of diffusion coefficient and relaxation time, the diffusion length. For both charge carriers can be determined. The values of the diffusion length for electrons and holes are found to be L_n = 9.16 x10^{-9} cm and L_p = 14.6 x10^{-9} cm, respectively. Our results are in good agreement with each other, since the mobility of holes is smaller compared with that of electrons, and its effective mass is larger than that of electrons. Its relaxation time will be larger than that of electrons. Figure 7 represens the dependence of TEP on carrier density for a given In_2Te_3 sample, as we have seen, α increases sharply and linearly with the increase of carrier concentration in the low carrier density region, and reaches a maximum value 165 μV /K at 1.1 x 10^{8} cm^{-3}. After that, the value of thermoelectric power decreases with the carrier density, α decreases gradually in the region of high carrier density. The general behavior of α as a function of P is quite similar to the temperature dependence of α. From this behavior we realize the effect of the charge carriers is a strong factor governing the variation α. The same behavior was observed when we plotted α *vs*. lnσ for In_2Te_3 sample as in Fg.8.

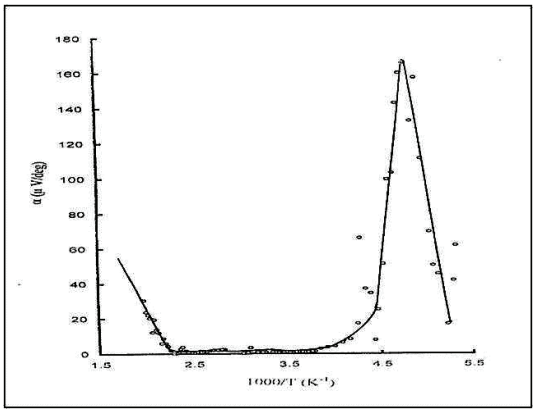

Fig. 7. Represens the dependence of TEP on carrier density for In_2Te_3 single crystal.

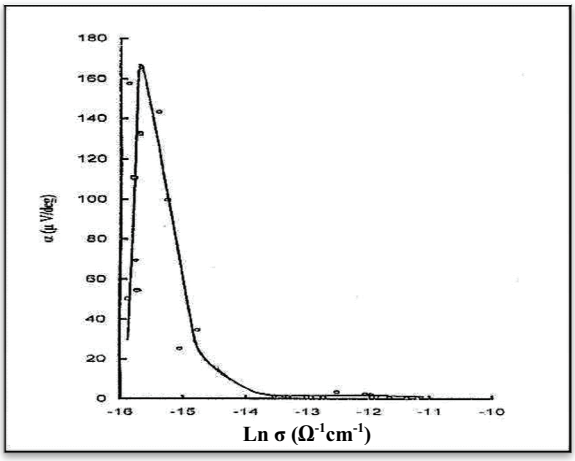

Fig. 8. The dependence of the thermoelectric power coefficient on the natural logarithm of the electrical conductivity for $In_2 Te_3$ single crystal.

This figure shows the dependence of thermoelectric power coefficient α on the natural logarithm of electrical conductivity according to[26]:

$$\alpha = \frac{K}{e}\left[A + \ln\frac{2\left(2\pi m_p^* KT\right)^{3/2} e\mu}{(2\pi h^3)}\right] - \frac{K}{e}\ln\sigma \qquad (4)$$

It is seen from the curve that the TEP decreases rapidly as the electrical conductivity increased in the lower conductivity reagion and decreased slowly with increasing conductivity in the higher conductivity region. Figure 8 also indicates that α no longer increases at conductivities higher than $1.5\text{x}10^{-7}$ Ω^{-1} cm^{-1}. From Fg.7.+8, we can deduce that the variation of α with the environmental temperature is not a mobility effect, but is dependent on the variation of the concentration. The choice of materials for thermoelectric generators and refrigerators is based on the efficiency parameter Z defined by the relation:

$$Z = \frac{\alpha^2 \sigma}{K} \qquad (5)$$

Where K is the thermal conductivity of a semiconductor, and σ is the electrical conductivity. This parameter was deduced and its value was found to be 1.3×10^{-7} K^{-1}. Indicating the efficiency of the material for conversion of thermal energy to electrical energy. The proposed

treatment of the experimental data sheds new light on the main physical parameters in In_2Te_3 single crystal. The pronounced parameters obtained from TEP data gave evidence for practical applications.

4- Conclusion

Measurements of electrical conductivity, Hall coefficient and TEP of In_2Te_3 single crystals are performed over wide range of temperature. The conductivity was found to be of P-type. The energy gap was calculated to be 0.99 eV. The electrical conductivity at room temperature is equal to $2.5x10^{-6}$ $\Omega^{-1}cm^{-1}$. The depth of the acceptor level is 0.3 eV. The hole mobility at room temperature was estimated as μ_p=1820 $cm^2V^{-1}sec^{-1}$ and electron mobility is equal to 2890 $cm^2V^{-1}sec^{-1}$. The effective masses of holes and electrons are $4.2x10^{-38}$ and $6.3x10^{-39}$ kg respectively. The diffusion coefficient for holes and electrons was evaluated to be 47 and 75 cm^2sec^{-1} respectively. The relaxation time was estimated for holes and electrons to be $4.5x10^{-18}$ sec and $1.2x10^{-18}$ sec respectively. The diffusion length for holes and electrons was found to be $14.6x10^{-9}$ cm and $9.16x10^{-9}$ cm respectively. Also the efficiency of the material as thermo-element was checked.

References

[1] **Aydogan, S., Karacah, T., Yogurtcu, Y.K.** (2005) *J. Cryst.growth* **279**: 110.
[2] **Nassary, M.M., Dongal, M., Gerges, M.K.** and **Sebuge, M.A.** (2003) *Phys. Stat. Sol*. (a) **199**: 404.
[3] **Emziane, M., Bernede, J.C., Ouerfelli, J., Essaidi, H.** and **Barreau A.** (1999) *Material chem and phys*. **61**: 229.
[4] **Zlomanov, V.P., Sheiman, M.S., Demin,V.N.** and **Legendre, B.J.** (2001) *Phase Equilibria* **22:** (1).
[5] **Okamoto, H.** and **White, C.E.T.** (1991) *Series Binary alloy phase Digrams* **338**.
[6] **Oh, C.S.** and **Lee, D.N.** (1993) *CALPHAD* **17**: 175.
[7] **Feutelais, Y.** and **Legendre, B.** (1998) *Thermochim Acta* **314:** 37.
[8] **Bose, D.N.** and **Purkayastha, S.** (1981) *De. Mat. Res. Bull.* **16:** 635.
[9] **Belal, A.E., Hussein, S.A., Madkour, H.** and **EL-Shikh, H.A.** (1993) *Indium J. Pure and Appl. Phys*. **31**: 464.
[10] **Balevicius, S., Cesnys, A.** and **Deksnys, A.** (1976) *Phy. Stat. Sol*. (a) **35**: 41.
[11] **Nassary, M.M., Hussein, S.A., Belal, A.E.** and **EL-Shaikh, H.A.** (1994) *Phys. Stat. Sol.* (a) **145:** 151.
[12] **Zaslavskiin, A.I., Kartenko, N.F.** and **Karach entseva, Z.A.** (1972) *Soviet phys. Solid stat,* **13:** 2152.
[13] **Jung, A.L., Situ, H., Lu, Y.W., Wang, Z.T.** and **He, Z.G.** (1989) *J. Non-cryst.Sol*. **114**: 115.
[14] **Finkman, E., Tauc, J.** (1975) *Physical Review Letters* **14**: 89.
[15] **Finkman, E., Tauc, J., Kershaw, R.** and **Wold, A.** (1975) *Physical Review* (B) **10**: 3785.

[16] **Koshkin, V.M., Galchinetskii, L.B., Kulik, V.N., Minkov, B.I.** and **Ulmanis, U.A.** (1973) *Sol. Stat. Comm*. **13:** 1.
[17] **Bleris, G.L., Karakostas, T., Stoemenos, J.** and **Economou, N.A.** (1976) *Phys. Stat. Sol*. (a) **34**: 243.
[18] **Sen, S.** and **Bose, D.N.** (1984) *Sol. Stat. Comm*. **50**: 39.
[19] **Hussein, S.A.** and **Nagat, A.T.** (1989) Cryst. *Res.Technal,* **24**: 283.
[20] **Hussein, S.A.** (1989) *Cryst. Res.Technal,* **24**: 635.
[21] **Hussein, S.A., Nagat, A.T., Gameel, Y.H.** and **Belal, A.T.** (1988) *Egypt. J. Solids* **10**: 45.
[22] **Guizzeffi, G., Meloni, F.** and **Baldereshi, A.** (1980) *15th-Int Conf, Phys, of semicnd, Kyoto*, **93** (1980).
[23] **Belal, A.E., Hussein, S.A., Madkour, H.** and **EL-Shaikh, H.A.** (1993) *Asion. J. Chem*. **5**: 644.
[24] **Johnson, V.A.** and **Lark, K.** (1953) *Phys Rev* **92**: 2.
[25] **Wilson, A.H.** (1953) *Theory of metals,* 2nd ed., Cambridge University press, Cambridge.
[26] **Schmid, P.H.E.** and **Mooser E.** (1972) *Helv,Phys. Acta*. **45**: 870.

الملامح المميزة والخصائص الانتقالية للمركب ثنائي الإنديوم – ثلاثي التليريوم أحادي التبلر

فاطمة سالم باهبري، ورقية حسين العريني

كلية العلوم للبنات، قسم الفيزياء، جامعة الملك عبدالعزيز

جدة – المملكة العربية السعودية

المستخلص. في هذه الدراسة تم تحضير المركب ثنائي الإنديوم – ثلاثي التليريوم في صورة أحادية التبلر، باستخدام تصميم محلي بسيط يمتاز بالكفاءة العالية ورخص تكلفته اعتمادًا على تقنية بريجمان للإنماء البلوري من المصهور. وتم التعرف على العينات المحضرة وتحديد درجة بلورتها وخلوها من وجود أطوار أخرى، وأنها على درجة عالية من النقاوة، باستخدام تقنية حيود الأشعة السينية. استخدمت البلورات المحضرة في قياسات الموصلية الكهربائية وظاهرة هول والقدرة الكهروحرارية، وذلك في مدى واسع من درجات الحرارة تحت تفريغ مناسب. أظهرت نتائج القياسات أن المركب يسلك سلوك شبه الموصل، وأن موصليته من النوع الموجب. كما تم تحديد اتساع النطاق المحظور وعمق مستوى الشوائب المستقبلة. كما أمكن تعيين الثوابت الرئيسية التالية: انسياقية حوامل التيار والكتلة الفعالة لحوامل التيار، ومعامل الإنتشار، وطول مسار الانتشار، وزمن الاسترخاء، وتركيز حوامل التيار، لكل من الثقوب والالكترونات. كما تم التعرف على كفاءة المركب لاستخدامه كعنصر كهروحراري، وعن طريق تحديد تلك العناصر الفيزيائية الهامة يمكن التعرف على المجال التطبيقي المناسب في التقنيات الحديثة، وخاصة في الدارات المتكاملة وكعناصر محولة للطاقة الحرارية إلى طاقة كهربائية.